



TECHNICAL REPORT RDMR-WD-16-48

STRAIN IMAGING USING TERAHERTZ WAVES AND METAMATERIALS

Henry O. Everitt and Martin S. Heimbeck
Weapons Development and Integration Directorate
Aviation and Missile Research, Development,
and Engineering Center

And

Willie D. Caraway
Science and Engineering Apprenticeship Program
College Qualified Leaders

And

Jonathan T. Richard
IERUS Technologies
2904 Westcorp Blvd. SW, Suite 210
Huntsville, AL 35805

And

**Christopher M. Bingham, Antonio Llopis,
and Nan M. Jokerst**
Department of Electrical and Computer Engineering
Duke University
Durham, NC 27708

November 2016

Distribution Statement A: Approved for public release; distribution is unlimited.



DESTRUCTION NOTICE

FOR CLASSIFIED DOCUMENTS, FOLLOW THE PROCEDURES IN DoD 5200.22-M, INDUSTRIAL SECURITY MANUAL, SECTION II-19 OR DoD 5200.1-R, INFORMATION SECURITY PROGRAM REGULATION, CHAPTER IX. FOR UNCLASSIFIED, LIMITED DOCUMENTS, DESTROY BY ANY METHOD THAT WILL PREVENT DISCLOSURE OF CONTENTS OR RECONSTRUCTION OF THE DOCUMENT.

DISCLAIMER

THE FINDINGS IN THIS REPORT ARE NOT TO BE CONSTRUED AS AN OFFICIAL DEPARTMENT OF THE ARMY POSITION UNLESS SO DESIGNATED BY OTHER AUTHORIZED DOCUMENTS.

TRADE NAMES

USE OF TRADE NAMES OR MANUFACTURERS IN THIS REPORT DOES NOT CONSTITUTE AN OFFICIAL ENDORSEMENT OR APPROVAL OF THE USE OF SUCH COMMERCIAL HARDWARE OR SOFTWARE.

REPORT DOCUMENTATION PAGE			Form Approved OMB No. 074-0188	
Public reporting burden for this collection of information is estimated to average 1 hour per response, including the time for reviewing instructions, searching existing data sources, gathering and maintaining the data needed, and completing and reviewing this collection of information. Send comments regarding this burden estimate or any other aspect of this collection of information, including suggestions for reducing this burden to Washington Headquarters Services, Directorate for Information Operations and Reports, 1215 Jefferson Davis Highway, Suite 1204, Arlington, VA 22202-4302, and to the Office of Management and Budget, Paperwork Reduction Project (0704-0188), Washington, DC 20503				
1. AGENCY USE ONLY		2. REPORT DATE November 2016		3. REPORT TYPE AND DATES COVERED Final
4. TITLE AND SUBTITLE Strain Imaging Using Terahertz Waves and Metamaterials				5. FUNDING NUMBERS
6. AUTHOR(S) Henry O. Everitt, Martin S. Heimbeck, Willie D. Caraway, Jonathan T. Richard, Christopher M. Bingham, Antonio Llopis, and Nan M. Jokerst				
7. PERFORMING ORGANIZATION NAME(S) AND ADDRESS(ES) Commander, U.S. Army Research, Development, and Engineering Command ATTN: RDMR-WDI-WSD Redstone Arsenal, AL 35898-5000				8. PERFORMING ORGANIZATION REPORT NUMBER TR-RDMR-WD-16-48
9. SPONSORING / MONITORING AGENCY NAME(S) AND ADDRESS(ES)				10. SPONSORING / MONITORING AGENCY REPORT NUMBER
11. SUPPLEMENTARY NOTES				
12a. DISTRIBUTION / AVAILABILITY STATEMENT Approved for public release; distribution is unlimited.				12b. DISTRIBUTION CODE A
13. ABSTRACT (Maximum 200 Words) Results are presented of an experimental polarimetric technique to measure strain in opaque objects. Experiments were conducted utilizing metamaterials on polydimethylsiloxane (PDMS) sheets to produce strain-induced birefringence at terahertz frequencies. Preliminary measurements are encouraging and show a qualitative agreement with theoretical predictions.				
14. SUBJECT TERMS Birefringence, Terahertz Waves, Metamaterials				15. NUMBER OF PAGES 16
				16. PRICE CODE
17. SECURITY CLASSIFICATION OF REPORT UNCLASSIFIED	18. SECURITY CLASSIFICATION OF THIS PAGE UNCLASSIFIED	19. SECURITY CLASSIFICATION OF ABSTRACT UNCLASSIFIED		20. LIMITATION OF ABSTRACT SAR

NSN 7540-01-280-5500

Standard Form 298 (Rev. 2-89)
Prescribed by ANSI Std. Z39-18
298-102

TABLE OF CONTENTS

	<u>Page</u>
I. INTRODUCTION	1
II. APPROACH.....	1
III. CONCEPT.....	4
IV. EXPERIMENTATION	5
V. RESULTS	7
VI. CONCLUSIONS.....	10
VII. FUTURE EFFORTS	10
LIST OF ABBREVIATIONS, ACRONYMS, AND SYMBOLS	11

LIST OF ILLUSTRATIONS

<u>Figure</u>	<u>Title</u>	<u>Page</u>
1.	Strain in Rod	1
2.	Object in Unpolarized Light	2
3.	Object in Polarized Light	2
4.	Woollam THz-VASE™ Model 1.00 Ellipsometer	3
5.	Electromagnetic Spectrum	4
6.	Metamaterials	5
7.	500 μm Region of Sample MM6 for uu Polarization	7
8.	500 μm Region of Sample MM6 for ux Polarization	8
9.	500 μm Region of Sample MM6 Mueller Matrix Prediction for ux Transmission	8
10.	500 μm Region of Sample MM7 for ux Polarization	9
11.	500 μm Region of Sample MM7 Mueller Matrix Prediction for ux Transmission	10

I. INTRODUCTION

Strain, the fraction by which an object is stretched or compressed, is an important engineering concern. Strain is illustrated in Figure 1, and the equation shows that strain is defined as the percent change in length. Also, notice how the strain has altered the rod's thickness, thereby changing and likely reducing its strength. Excess strain degrades structural integrity and is often the cause of structural failure. Currently, no method exists for measuring strain in opaque objects. The discovery of a method for determining strain would allow engineers to measure the strain and create strain maps that would reveal which parts of the object are under the greatest strain. Engineers could assess whether the strain is sufficiently great to present a structural problem and take appropriate action to eliminate or minimize the problem. The ability to create strain maps is important because the maps would greatly assist engineers in creating more reliable devices. For example, failure of a helicopter rotor blade could be catastrophic. The ability to map the strain in the blade would allow engineers to design blades that would be less likely to fail. Strain mapping would also allow engineers to determine whether damage, such as cracks, was minor or severe by determining whether excess strain was developing around the damaged area.

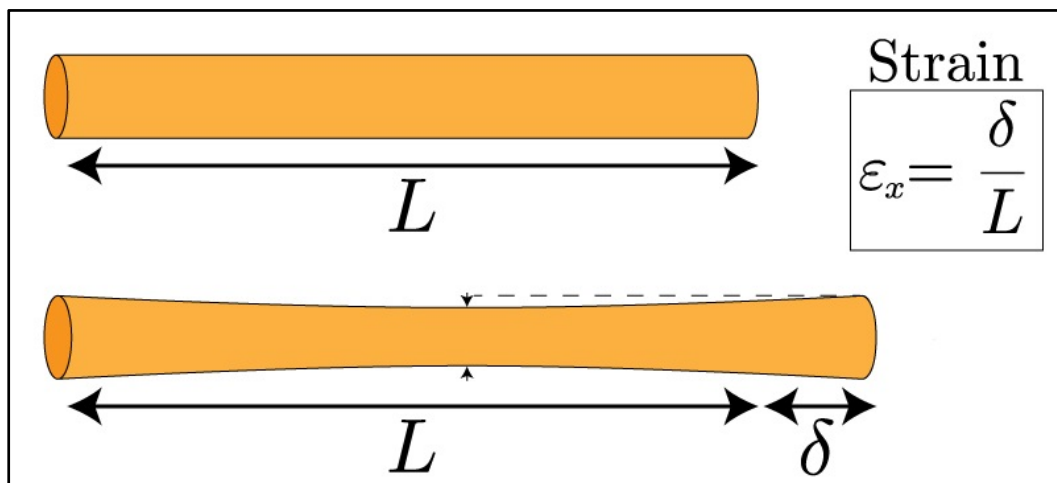


Figure 1. Strain in Rod

II. APPROACH

While no method exists for the measurement of strain in opaque objects, a technique for the measurement of strain in transparent objects is available. In this technique, visible light is passed through a transparent object, and the intensity and polarization of the exiting light are measured. This technique is known as visual-light-based strain-birefringence testing, and a strain map is illustrated in Figures 2 and 3. Figure 2 shows half of a plastic tape holder exposed to normal lighting (that is, unpolarized light), while Figure 3 depicts the same plastic tape holder exposed to polarized light. Notice how different strain levels appear as different colors, creating a map of the strain in the object. Also notice how some cracks are revealed to noticeably alter the strain, while others have no appreciable effect.



Figure 2. Object in Unpolarized Light

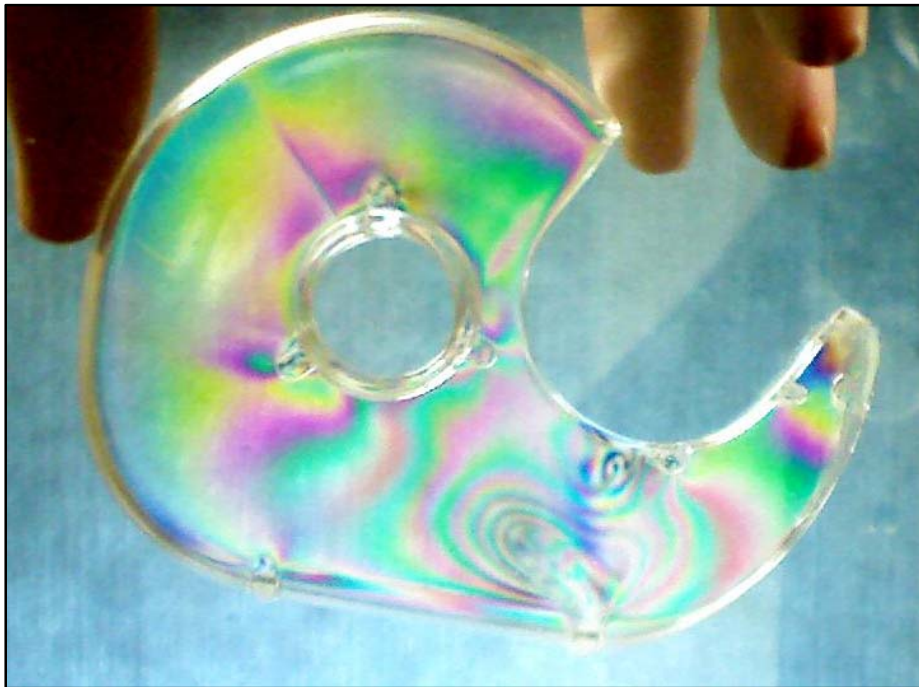


Figure 3. Object in Polarized Light

Birefringence is the property of affecting differently the different polarizations of Electromagnetic (EM) waves. A birefringent material usually changes the polarization of incident EM waves by favoring the transmission of waves of a particular polarization. The interaction of some materials with incident light is dependent upon the strain experienced by the materials, and materials exhibiting this property are said to exhibit strain-induced birefringence.

To test an object's interaction with light, an ellipsometer is often used. An ellipsometer, such as the one manufactured by the J. A. Woollam Company and shown in Figure 4, is a device capable of producing EM waves at defined frequencies and polarizations and measuring the intensity and polarization of the waves after they have passed through the test material or object. Using the measured transmission intensity values, the ellipsometer can calculate, among other things, the Mueller matrix of the test material or object. The Mueller matrix quantifies the effects of alterations in the intensity and polarization of light passing through an object. The Mueller matrix is a property of the object and frequency dependent.



Figure 4. Woollam THz-VASE™ Model 1.00 Ellipsometer

For objects composed of materials that exhibit strain-induced birefringence, a model can be created describing the Mueller matrix of the object in terms of both frequency and strain. Light can then be passed through a transparent object at a frequency at which the Mueller matrix is noticeably different for different strain values. The intensity and polarization of the exiting light can then be measured and used to calculate the strain level. This process, known as visual-light-based strain-birefringence testing, is the test used for measuring strain in transparent objects.

Visual-light-based strain-birefringence testing cannot be used for opaque materials because this test requires that light be transmitted by the object being tested. Opaque materials do not transmit light. However, the EM spectrum is far more extensive than the relatively tiny visible light band. This project investigates the use of an experimental polarimetric technique to measure the strain in opaque objects by using the principles of strain-induced birefringence.

III. CONCEPT

To overcome the inability of visual light to penetrate opaque objects, terahertz radiation was investigated. Longer wavelength EM waves, such as radio waves, have excellent penetration ability but low image resolution. Shorter wavelength EM waves, such as visual light, have poor penetration ability but produce high-resolution images. However, the terahertz band illustrated in Figure 5 that is located in the high-frequency portion of the microwave band and low-frequency portion of the infrared band exists in a transition region in the EM continuum within which the properties of shorter wavelength waves progress into the properties of longer wavelength waves. Terahertz waves are high-frequency microwaves with frequencies between approximately 0.3 and 3 terahertz. By using terahertz radiation for strain-birefringence testing, it is possible to tune the frequency being used to gain greater penetration of the object when necessary or to reduce excess penetration in favor of greater resolution.

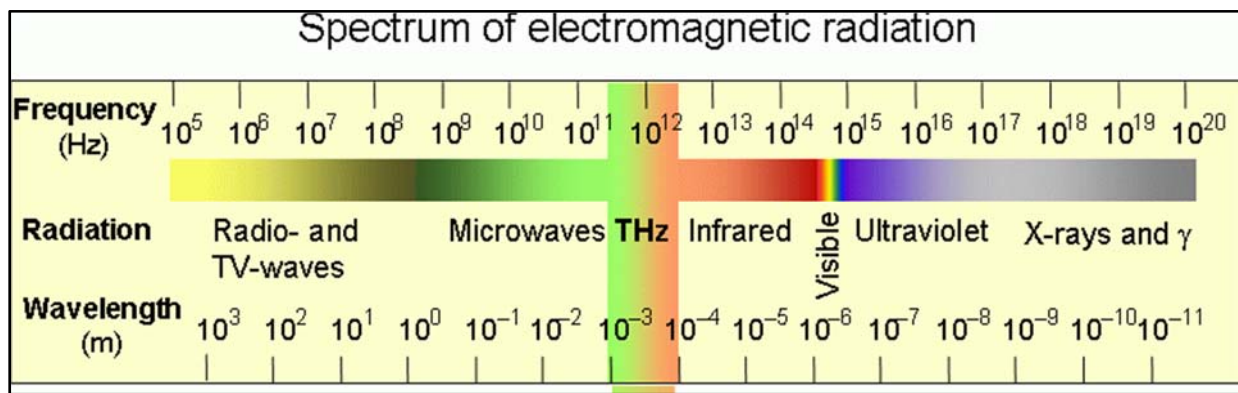


Figure 5. Electromagnetic Spectrum

Because terahertz radiation has a longer wavelength than visible light, larger changes in the material or object being tested are needed to show the effects of strain. In strain-induced birefringence in the visible-light frequencies, strain causes the atoms or molecules that comprise the object to be pulled and pushed relative to one another, leading to changes in the distances between them. These atomic movements change the Mueller matrix of the material, thus changing how the object interacts with incident light. However, these minuscule changes are too small to produce a discernible impact in the interaction of the object with terahertz radiation. Therefore, metamaterials are affixed to the object to be tested.

Metamaterials are a class of materials designed to have combinations of properties that are not normally found in nature. For this project, the metamaterials used are metal pieces that were chosen for their inductive and capacitive properties. These metamaterials are depicted in Figure 6, which is an image of the metamaterials used in this project taken using a microscope with a lens magnification of 200x. When EM waves from a particular range of frequencies (determined by the spacing between the metamaterials) strike the metamaterials, resonance occurs and changes how the waves are transmitted. By stretching the metamaterials and the distance between them, the frequency at which resonance occurs is changed. The metamaterials function as artificial atoms and cause changes in the Mueller matrix for the object to which the metamaterials are affixed.

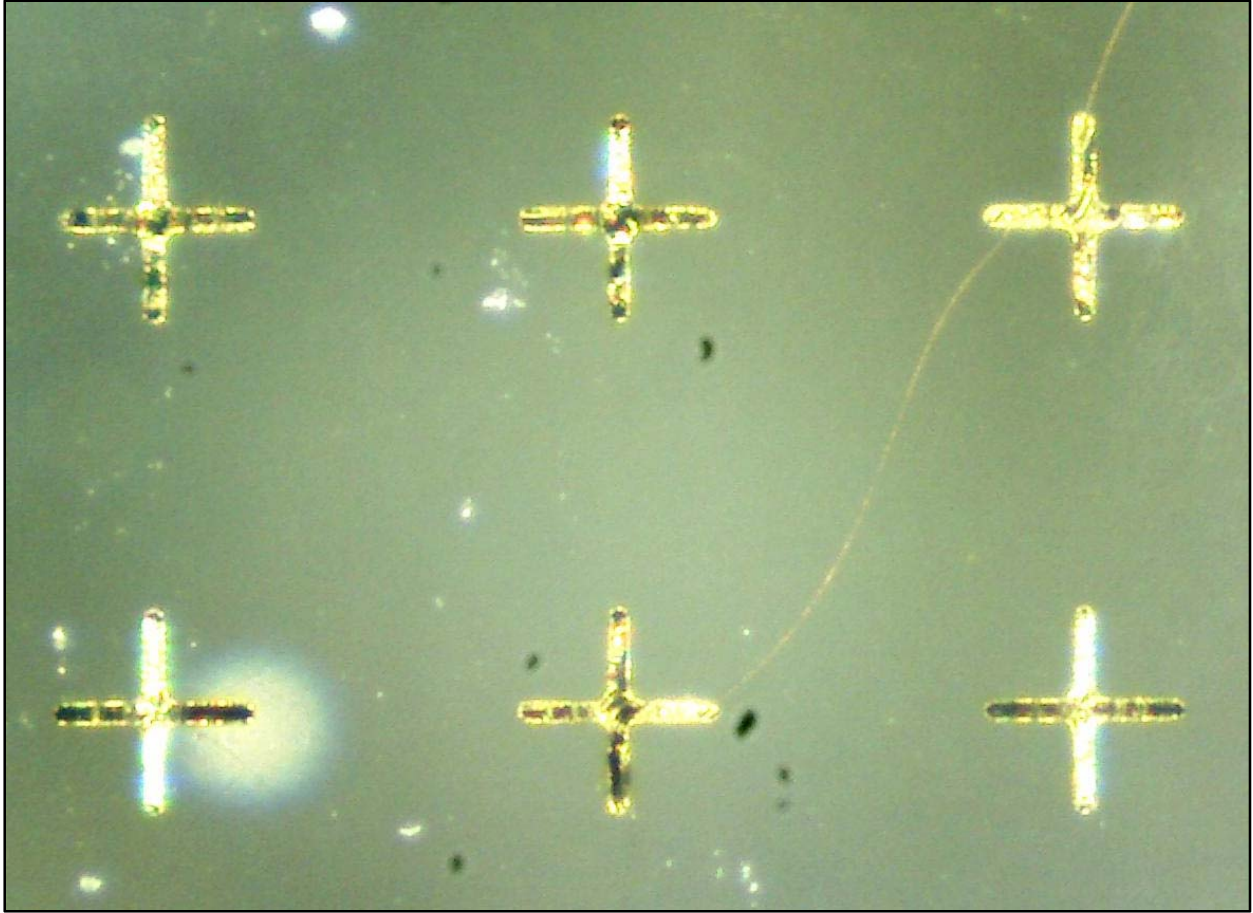


Figure 6. Metamaterials

IV. EXPERIMENTATION

To test the terahertz-based strain-birefringence method for measuring the strain in opaque materials, samples of polydimethylsiloxane (PDMS), a silicone compound similar to rubber, were examined. Thin sheets of PDMS were obtained, and layers of metamaterials were affixed to the front of the sheets. Sample MM6 contains a single layer of metamaterials, while sample MM7 contains two layers of metamaterials. Each layer of metamaterials was divided into four regions based on the distance between the metamaterials. If the sample had two layers of metamaterials, the regions were aligned so that incident radiation must pass through two regions with the same properties. The four regions were a baseline region with no metamaterials (a control case) and three regions with metamaterials spaced 500, 750, and 1,000 microns (μm) apart. The region of interest is the 500 μm region, since the 750 and 1,000 μm regions do not have resonance frequencies in the frequency range tested. Therefore, all measurements were made on the 500 μm regions but not necessarily on the 750 or 1,000 μm regions. The samples were mounted in a bracket that could stretch them vertically with gradations to measure the amount by which they were stretched. For this experiment, the samples were subjected to 0, 2, 4, and 6-percent (%) strain.

These samples were tested in a Woollam THz-VASE™ Model 1.00 Ellipsometer. Using frequencies of 330 to 500 gigahertz (GHz), the Mueller matrices were measured for each region of each sample. In addition, the transmission of terahertz radiation of the indicated frequencies of various polarizations was measured for each region of each sample. Measurements were taken at increments of 1 GHz. Each measurement was taken 10 times and then averaged to produce a single data point. Transmission measurements through the baseline region were used as a reference, and transmission measurements through the other regions were divided by the reference value for that frequency and strain level. Strain was applied along the vertical axis of each sample.

One test of particular note was the measurement of transmission using cross polarizers. In this test, incident radiation is polarized at an angle of +45 degrees relative to the horizontal, transmitted through the sample, transmitted through a polarizer that allows only -45 degree polarized radiation to pass, and then measured by the detector. Because +45 degree polarized radiation has no -45 degree polarized component (since the two differ by 90 degrees), no radiation will reach the detector unless the sample rotates the polarization. This transmission measurement can be verified by using the Mueller matrix. Where M_{+45} is the Mueller matrix of the +45 degree polarizer, M_{sample} is the Mueller matrix of the sample, M_{-45} is the Mueller matrix of the -45 degree polarizer, and S is the radiation before it reaches the first polarizer (the design of the ellipsometer has already polarized this radiation to +45 degrees), the radiation reaching the detector can be found to have the following vector form.

$$\begin{aligned}
M_{-45}M_{sample}M_{+45}S &= \begin{bmatrix} \frac{1}{2} & 0 & -\frac{1}{2} & 0 \\ 0 & 0 & 0 & 0 \\ -\frac{1}{2} & 0 & \frac{1}{2} & 0 \\ 0 & 0 & 0 & 0 \end{bmatrix} \begin{bmatrix} m_{11} & m_{12} & m_{13} & m_{14} \\ m_{21} & m_{22} & m_{23} & m_{24} \\ m_{31} & m_{32} & m_{33} & m_{34} \\ m_{41} & m_{42} & m_{43} & m_{44} \end{bmatrix} \begin{bmatrix} \frac{1}{2} & 0 & \frac{1}{2} & 0 \\ 0 & 0 & 0 & 0 \\ \frac{1}{2} & 0 & \frac{1}{2} & 0 \\ 0 & 0 & 0 & 0 \end{bmatrix} \begin{bmatrix} 1 \\ 0 \\ 1 \\ 0 \end{bmatrix} \\
&= \begin{bmatrix} \frac{1}{2}(m_{11} - m_{31}) & \frac{1}{2}(m_{12} - m_{32}) & \frac{1}{2}(m_{13} - m_{33}) & \frac{1}{2}(m_{14} - m_{34}) \\ 0 & 0 & 0 & 0 \\ \frac{1}{2}(-m_{11} + m_{31}) & \frac{1}{2}(-m_{12} + m_{32}) & \frac{1}{2}(-m_{13} + m_{33}) & \frac{1}{2}(-m_{14} + m_{34}) \\ 0 & 0 & 0 & 0 \end{bmatrix} \begin{bmatrix} \frac{1}{2} & 0 & \frac{1}{2} & 0 \\ 0 & 0 & 0 & 0 \\ \frac{1}{2} & 0 & \frac{1}{2} & 0 \\ 0 & 0 & 0 & 0 \end{bmatrix} \begin{bmatrix} 1 \\ 0 \\ 1 \\ 0 \end{bmatrix} \\
&= \begin{bmatrix} \frac{1}{4}(m_{11} - m_{31} + m_{13} - m_{33}) & 0 & \frac{1}{4}(m_{11} - m_{31} + m_{13} - m_{33}) & 0 \\ 0 & 0 & 0 & 0 \\ \frac{1}{4}(-m_{11} + m_{31} - m_{13} + m_{33}) & 0 & \frac{1}{4}(-m_{11} + m_{31} - m_{13} + m_{33}) & 0 \\ 0 & 0 & 0 & 0 \end{bmatrix} \begin{bmatrix} 1 \\ 0 \\ 1 \\ 0 \end{bmatrix} \\
&= \begin{bmatrix} \frac{1}{2}(m_{11} - m_{31} + m_{13} - m_{33}) \\ 0 \\ \frac{1}{2}(-m_{11} + m_{31} - m_{13} + m_{33}) \\ 0 \end{bmatrix} = \begin{bmatrix} a \\ 0 \\ -a \\ 0 \end{bmatrix}
\end{aligned}$$

From this result, it is apparent that the equation $a = \frac{1}{2}(m_{11}+m_{13}-m_{31}-m_{33})$, where a is the intensity of the transmitted radiation (all of which is at -45 degree polarization) and m_{xy} is the element in the x^{th} row and y^{th} column of the Mueller matrix, can be used to predict the transmission during a cross-polarization experiment. Because of the method that the ellipsometer uses to normalize the data, the predicted transmission may be a constant multiple of the actual transmission.

V. RESULTS

The test results reveal strain-induced birefringence in sample MM6 (500 μm region). The measurements of the Mueller matrix for sample MM6 reveal strain dependence in several of the matrix elements. In addition, the transmission of certain polarizations shows strain dependence, as shown in Figure 7. This figure illustrates the measurements of the amount of +45 degree polarized terahertz radiation exiting the 500 μm region of sample MM6 when the incident radiation was polarized to +45 degrees. It can be observed that the magnitude of the dip in transmission changes with strain and the frequency at which the dip is strongest also changes with strain. Cross-polarization measurements show no appreciable rotation of polarization, as shown in Figure 8, which is supported by the sample's Mueller matrix, as shown in Figure 9. Figure 8 plots the cross-polarization transmission measurements (measurements of how much -45 degree polarized terahertz radiation exited the sample when the incident radiation was polarized to +45 degrees) for the 500 μm region of sample MM6. These measurements indicate that the sample has a negligible ability to rotate the polarization of the sample. Figure 9 depicts the Mueller matrix prediction for cross-polarization transmission in the 500 μm region of MM6 calculated using the expression $\frac{1}{2}(m_{11}+m_{13}-m_{31}-m_{33})$, which supports the lack of polarization rotation in cross-polarized transmission measurements seen in Figure 8.

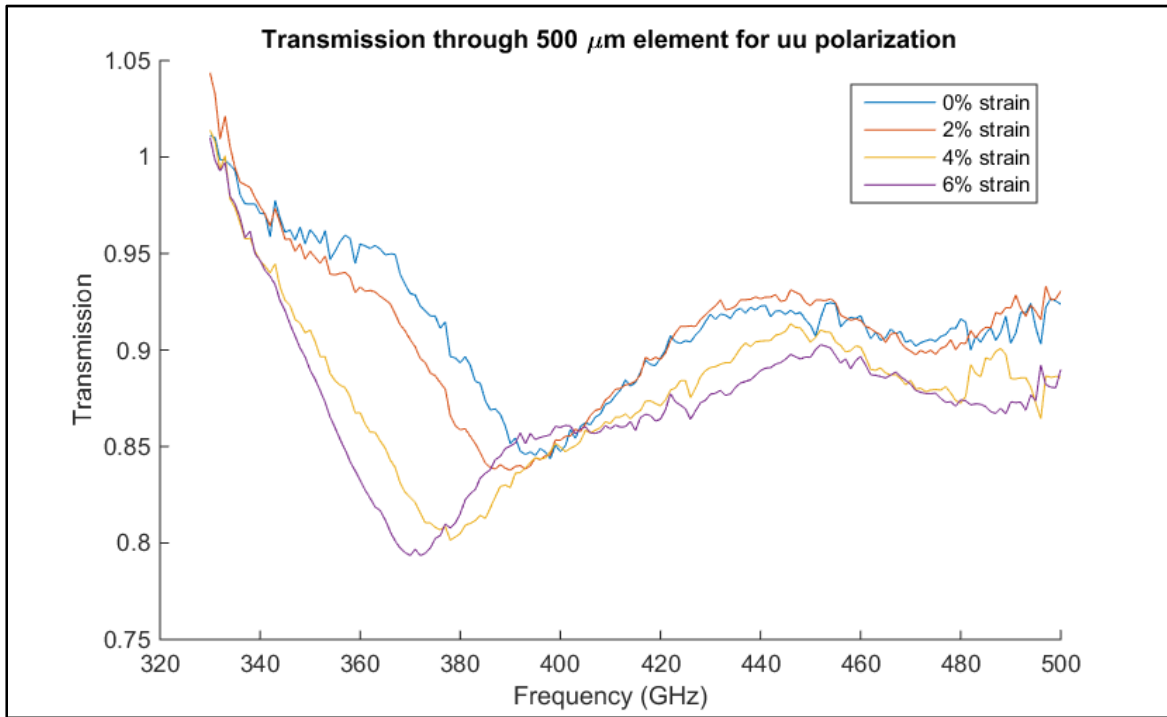


Figure 7. 500 μm Region of Sample MM6 for uu Polarization

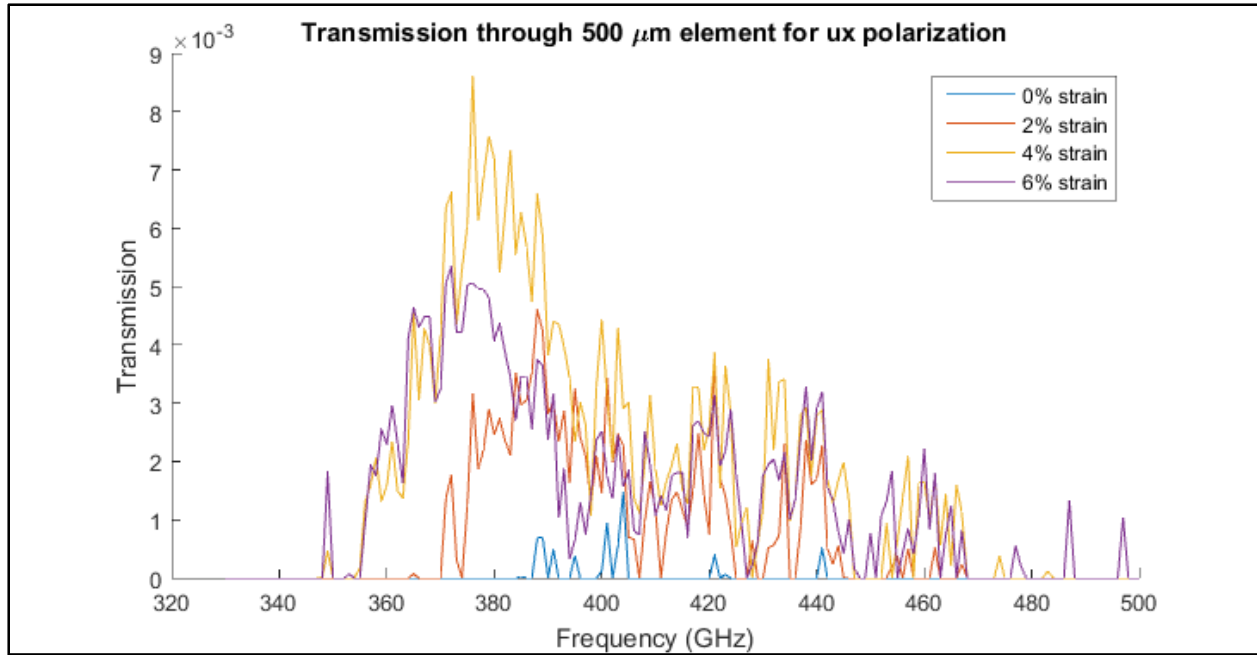


Figure 8. 500 μm Region of Sample MM6 for ux Polarization

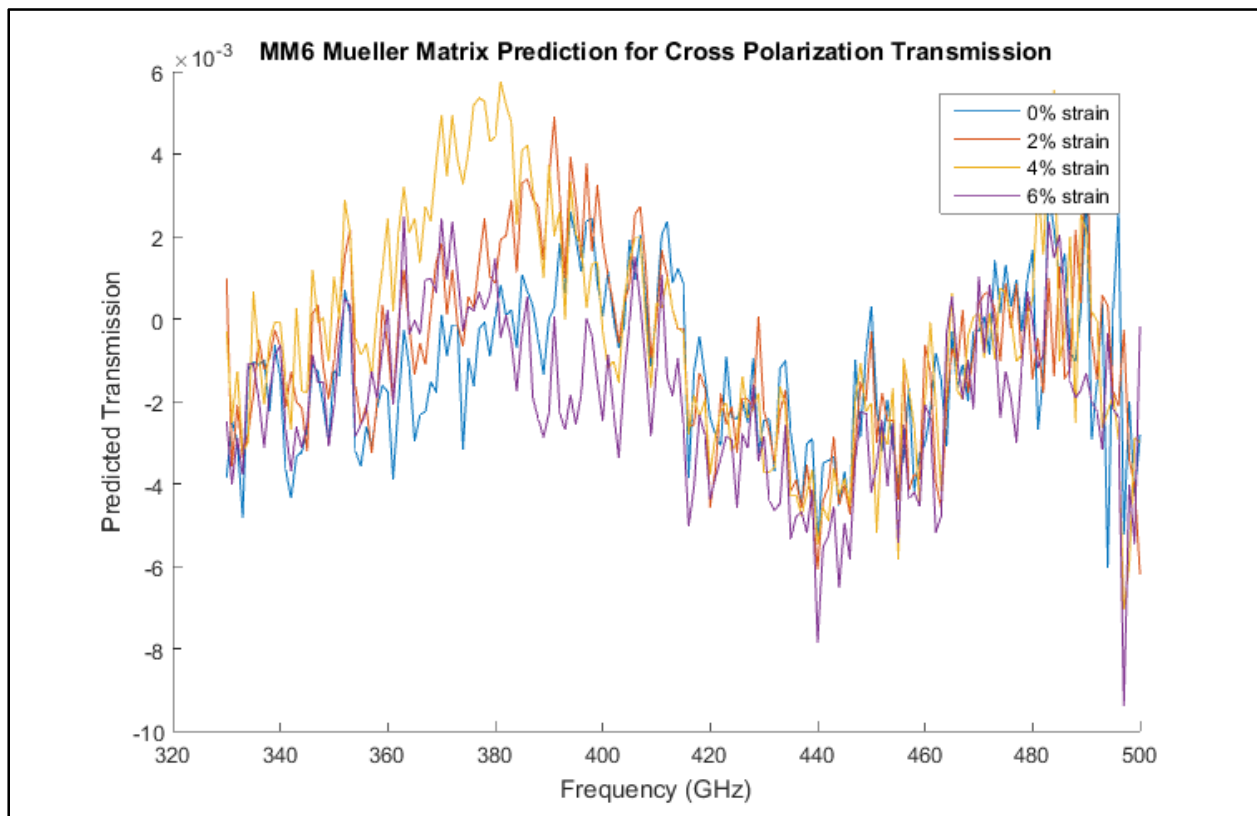


Figure 9. 500 μm Region of Sample MM6 Mueller Matrix Prediction for ux Transmission

Sample MM7 (500 μm region) exhibited a much greater degree of strain-induced birefringence than did sample MM6. The Mueller matrix of sample MM7 shows much greater strain dependence and variation across frequencies. Whereas the Mueller matrix of sample MM6 showed variation in only a few elements, most of the elements of the Mueller matrix of sample MM7 exhibited dependence upon frequency and strain. Also, the transmission measurements show strain dependence for more polarizations than did the transmission measurements of sample MM6. Of particular note, Figure 10, which plots the cross-polarization transmission measurements (measurements of how much -45 degree polarized terahertz radiation exited the sample when the incident radiation was polarized to +45 degrees) for the 500 μm region of sample MM7, shows that sample MM7 allowed transmission even when cross polarizers were used. Sample MM7's ability to allow transmission in this test reveals the sample's ability to rotate the polarization of incident terahertz waves, and the data show that this ability is strongly strain-dependent. This ability to rotate polarization and the strain dependence of this ability are both confirmed by the Mueller matrix, as shown in Figure 11. Figure 11 depicts the Mueller matrix prediction for cross-polarization transmission in the 500 μm region of MM7 calculated using the expression $\frac{1}{2}(m_{11}+m_{13}-m_{31}-m_{33})$.

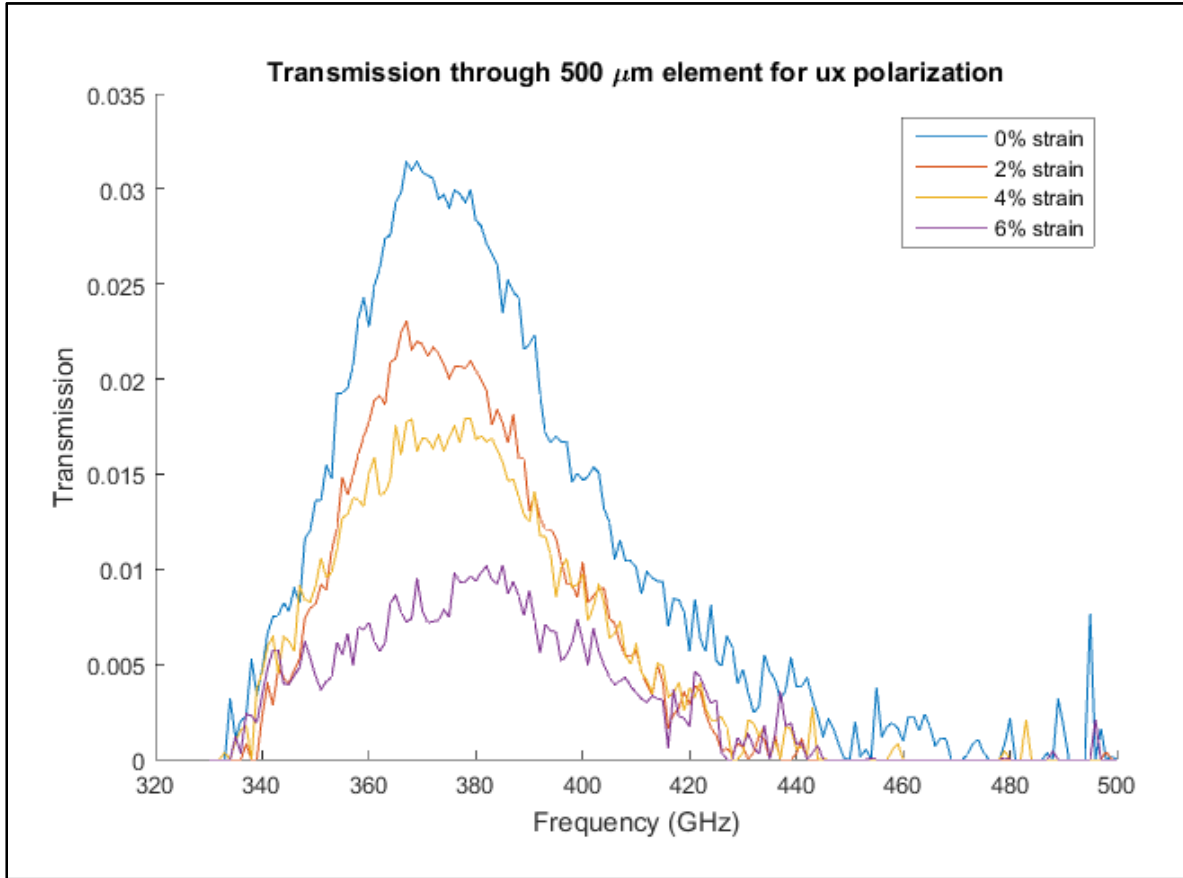


Figure 10. 500 μm Region of Sample MM7 for ux Polarization

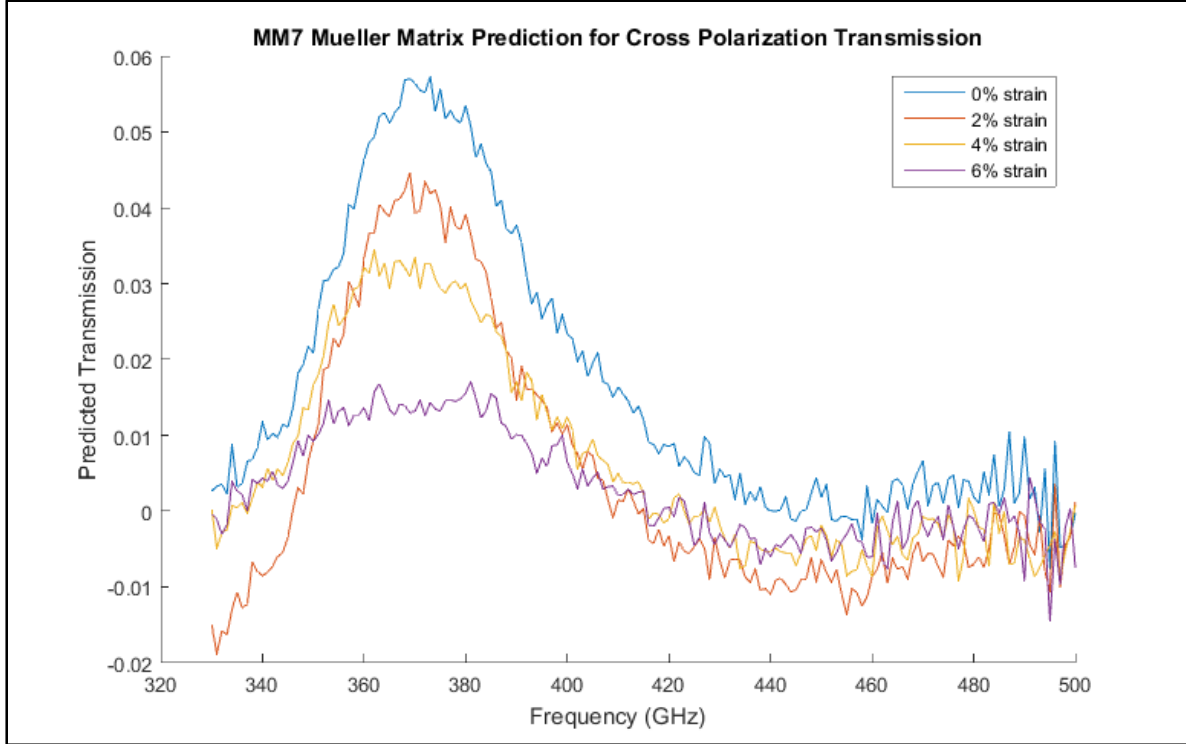


Figure 11. 500 μm Region of Sample MM7Mueller Matrix Prediction for u_x Transmission

The results confirmed that strain-induced birefringence can be seen at terahertz frequencies in objects to which metamaterials have been affixed and also confirmed several aspects of the birefringence. First, spacing between metamaterials of 500 μm proved more effective at exhibiting strain-induced birefringence than spacing of both 750 and 1,000 μm for the frequencies examined. A double layer of metamaterials proved more effective at generating strain-induced birefringence, but a single layer could be used. Fewer polarizations are affected by differences in strain for the single-layer sample than for the double-layer sample, and the double-layer sample is able to rotate the polarization of incident terahertz radiation, while the single-layer sample is not. These results agree qualitatively with theory.

VI. CONCLUSIONS

The application of metamaterials was effective in producing strain-induced birefringence at terahertz frequencies. Therefore, strain-birefringence testing at terahertz frequencies is a promising technique for the measurement of strain in opaque objects.

VII. FUTURE EFFORTS

An ability to collect measurements at many points within a sample object should be incorporated, possibly by incorporating automated motor movements into the sample mount, to allow a map of the strain in the object to be generated. Additional measurements should be taken using different sample materials to develop models relating strain to terahertz wave transmission in those other materials.

LIST OF ABBREVIATIONS, ACRONYMS, AND SYMBOLS

%	percent
EM	Electromagnetic
GHz	gigahertz
Hz	hertz
m	meter
PDMS	polydimethylsiloxane
THz	terahertz
x	times
δ	Symbol Representing Change in Length (Delta)
ϵ	Symbol Representing Strain (Epsilon)
μm	micrometer, micron